ORIGINAL ARTICLE

The fibulin-1 gene *(FBLN1)* is disrupted in a t(12;22) associated with a complex type of synpolydactyly

P Debeer, E F P M Schoenmakers*, W O Twal, W S Argraves, L De Smet, J-P Fryns, W J M Van de Ven

....

See end of article for authors' affiliations

....

Correspondence to:
Dr P Debeer, Centre for Human Genetics, Herestraat 49, B-3000 Leuven, Belgium;
philippe.debeer@med.kuleuven.ac.be

*Present address:
Department of Human Genetics, University Medical Centre Nijmegen, Nijmegen, The Netherlands

....

Molecular analysis of the reciprocal chromosomal translocation t(12;22)(p11.2;q13.3) cosegregating with a complex type of synpolydactyly showed involvement of an alternatively spliced exon of the fibulin-1 gene *(FBLN1* located in 22q13.3) and the *C12orf2 (HoJ-1)* gene on the short arm of chromosome 12. Investigation of the possible functional involvement of the fibulin-1 protein (FBLN1) in the observed phenotype showed that FBLN1 is expressed in the extracellular matrix (ECM) in association with the digits in the developing limb. Furthermore, fibroblasts derived from patients with the complex type of synpolydactyly displayed alterations in the level of FBLN1-D splice variant incorporated into the ECM and secreted into the conditioned culture medium. By contrast, the expression of the FBLN1-C splice variant was not perturbed in the patient fibroblasts. Based on these findings, we propose that the t(12;22) results in haploinsufficiency of the FBLN1-D variant, which could lead to the observed limb malformations.

The formation of digits is a complex, tightly regulated process which involves apoptosis and in which several pathways and signalling molecules are involved. The presentation of a small family with a very specific congenital hand malformation associated with an apparently balanced autosomal reciprocal translocation provided us with the opportunity to identify novel genes involved in limb development. Previously, we described the clinical phenotype of three patients from one family sharing a complex type of synpolydactyly (fig 1) associated with a constitutional balanced t(12;22)(p11.2;q13.3) and the exclusion of synpolydactyly associated *HOXD13* mutations in these patients.[1–3] All affected subjects carry the constitutional balanced translocation, whereas unaffected family members have a normal karyotype. The cosegregation of the phenotype with this translocation suggested that a synpolydactyly associated gene might be localised at one or both of the chromosomal breakpoints involved in this translocation. As a first step towards the identification of the genes involved in the translocation, we were able to pinpoint the breakpoint region on chromosome 12 to a 2.6 kb *Bam*HI fragment.[4]

Here, we describe the cloning of the translocation breakpoint and the identification of two genes directly targeted by this translocation. One of these genes, *FBLN1*, turned out to be the ideal positional and functional candidate for the observed phenotype. We therefore examined the consequences of the translocation induced disruption on the expression of *FBLN1-D*, one of the four variants of *FBLN1*, in the possible genesis of the limb malformations observed in our patients.

MATERIALS AND METHODS

Vectorette PCR
Vectorette PCR experiments were performed essentially as described by Schoenmakers *et al.*[5] Genomic DNA was digested with *Bam*HI and a vectorette linker with *Bam*HI compatible cohesive ends was ligated to the digested DNA. This ligated DNA was used in two consecutive rounds of (hemi-nested) PCR amplification. In a first round a universal vectorette primer (5′-CGAATCGTAACCGTTCGTACGAGAATCGCT-3′) was used in combination with a specific primer (5′-CTTGAAGGAGAGAGGCAGGGAAACTGAAGTGG-3′), based

on sequence data obtained during random sequence sampling, and mapping within the rearranged 2.6 kb *Bam*HI fragment on chromosome 12p. Part of the DNA produced in this first round was then reamplified using the same universal vectorette primer and the following (nested) chromosome 12 specific primer (5′-GGTAATGCATGCTACATGGTGGCTTCA GGG-3′). PCR products were analysed on, and recovered from, standard 1% agarose gels and subcloned using the pGEM-T Easy system (Promega).

Sequencing of the wild type *FBLN1-D* and construction of *FBLN1* probes
The sequence of the presumed wild type *FBLN1-D* was determined as follows: first, the wild type *FBLN1-D* cDNA was isolated with the *FBLN1-D* specific cDNA synthesis primer (5′-CCACCTATAAGAAAAGAT-3′). This primer is located downstream of the translocation breakpoint, so only the presumed wild type transcript, that is, originating from the non-disrupted gene, was isolated. Subsequently, overlapping fragments covering the whole *FBLN1-D* cDNA were amplified by PCR and subcloned in the pGEM-T Easy vector.

The following primer sets were used to amplify the overlapping cDNA fragments: RT1-up: 5′-CTCATTTTTAATGCG AAGGCTAAG-3′; RT1-low: 5′-AAGAAA AGATGGATGATG CAGAGTG-3′; RT2-up: 5′-TGCGGGACTCTTTTGACATCATC- 3′; RT2-low: 5′-TCTTTCTTTCCTTGGCCCTTAGC-3′; RT3-up: 5′-CGC AACTGCCAAGACATTGATGA-3′; RT3-low: 5′-CAGCTT CAGGACGGCATGAAATG-3′; RT4-up: 5′-AGAACACGCTGGG CTCCTACCTC-3′; RT4-low: 5′-CGGACCGTGTCTGTCTTCT CCTG-3′; RT5-up: 5′-GCCCTATTGGGCATACATGCATC-3′; RT5-low: 5′-CTCGCCGGCAGTAACACTGGTAG-3′; RT6-up: 5′-GACGAGGTGGTCTGCTCCTGCTT-3′; RT6-low: 5′-CGCACT CGTCCACATCAACACAG-3′; RT7-up: 5′-TCAAGAGCC AGGAGACCGGAGA-3′; RT7-low: 5′-CTGGTAGCCCACGAA GCAGGAG-3′; RT8-up: 5′-CCCGCCGCCCATGGAGCGCGC-3′; RT8-low: 5′-CGGCACTGCTGCTTGCAGGGCCCGC-3′.

....
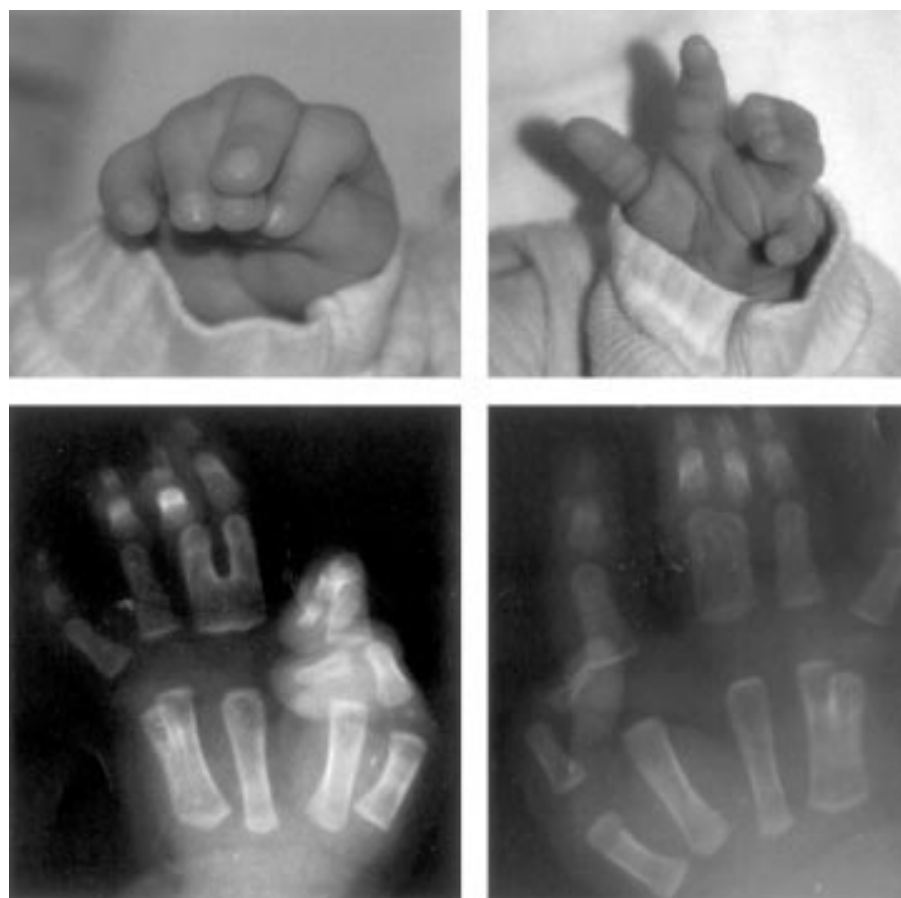
Figure 1 Clinical and radiological appearance of the hand malformations associated with the t(12;22).

Annealing temperatures of 60°C were used for all primer combinations. DMSO (10% final concentration) was added when using sets RT5, RT7, and RT8. Sequencing was performed using standard protocols and T7 and SP6 primers.

FBLN1 probes for northern blot analysis were constructed by PCR. The *FBLN1-D* specific probe was amplified using primers 5′-ACCATCTCCCACA-3′ (position 1793-1805 in *FBLN1-D* mRNA) and 5′-CAGCAATGATTTG-3′ (position 2162-2174). Similarly, a *FBLN1-C* specific probe was constructed using primers 5′-CCAAGCTGCCTCTGAGAATA-3′ (position 1749-1768 in *FBLN1-C* mRNA) and 5′-GCTCTGCAGACACAAAGATG-3′ (position 2038-2057). For the probe residing within the part common to all *FBLN1* variants, primers RT5-up and RT5-low were used.
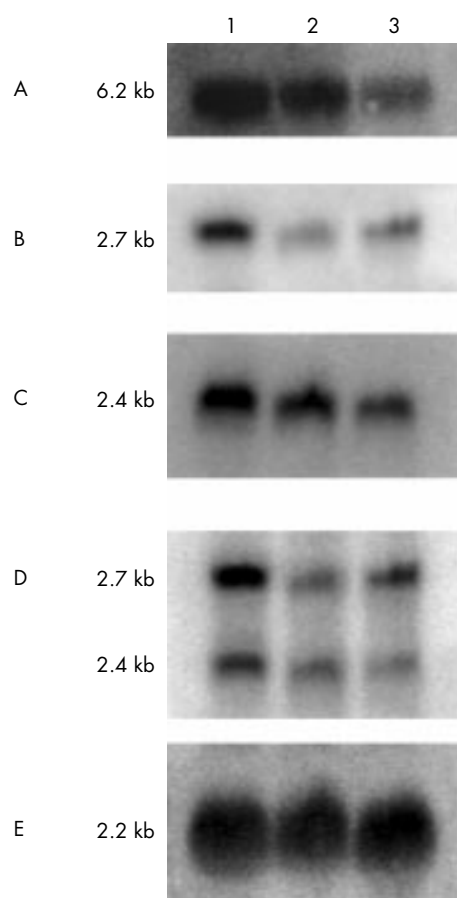
3′ RACE analysis

3′ RACE was performed according to the method described by Schoenmakers *et al*[6] with minor modifications. RNA used for the 3′ RACE analysis was derived from skin fibroblasts. First strand cDNA synthesis was performed using the poly (A) specific primer AP2 (5′-AAGGATCCGTCGACATC(T)$_{17}$-3′) or a *FBLN1-D* specific primer (5′-CCACCTATAAGAAAAGAT-3′). Specific 3′ RACE primers were designed on the published *FBLN1-D* sequences. In the first PCR round, a specific *FBLN1-D* primer (5′-CCAACGATGTCACATGCGTGT-3′, position 1760-1780 in *FBLN1-D* mRNA), located in the first *FBLN1-D* specific exon (exon 18) was used in combination with the AP2 specific primer UAP2 (5′-CUACUACUACUAAAGGATCCGTCGACATC-3′). In the second round, a tailed, nested primer (5′-CAUCAUCAUCAUAAGGATCCGTCGACA-3′, position 1795-1808), also situated within the first *FBLN1-D* specific exon (exon 18) was used in combination with the UAP2 primer.

Detection of fibulin-1 in conditioned culture medium and extracellular matrix of cultured fibroblasts

Age matched, normal foreskin fibroblasts (ATCC CRL 2056, Rockville, MD) and synpolydactyly fibroblasts isolated from skin biopsy (obtained during surgery after informed consent) were grown in 100 mm tissue culture plates (Corning, Corning, NY) in Dulbecco's Minimal Essential medium (DMEM) supplemented with 10% iron supplemented bovine calf serum (Hyclone, Logan, UT) until they reached 90% confluency. The medium was then aspirated and replaced with DMEM supplemented with insulin, transferrin, and selinious acid (5 µg/ml, 5 µg/ml, and 5 ng/ml, respectively, Becton Dickinson Labware Bedford, MA). After an additional three days in culture, the conditioned culture medium (CCM) was collected and the cell layer washed with phosphate buffered saline (pH 7.4). The cell layer was then extracted with 10 mmol/l EDTA for five minutes with gentle agitation. The extraction buffer was collected and centrifuged for 10 minutes at 2000 × g. A 400 µl aliquot of the supernatant was concentrated with 10 µl of Strataclean resin (Stratagene, La Jolla, CA) by vortexing for one minute and centrifugation at 13 000 × g for 10 seconds. Similarly, a 500 µl aliquot of CCM was absorbed with Strataclean resin and 10 µl of 2 × Laemmli sample buffer containing β-mercaptoethanol was added to each sample and extracts were run on SDS-PAGE using 4-20% gels (Invitrogen/Novex, Carlsbad, CA). After SDS-PAGE, proteins were transferred to PVDF membrane and probed with antibodies against FBLN1 (1 µg/ml) in Tris buffered saline (pH 7.4) containing 0.1% Tween 20 and 5% non-fat milk. Bound antibody was detected using horseradish peroxidase (HRP) labelled secondary antibody (1:5000 dilution, Amersham Pharmacia, Piscataway, NJ) and ECL+ detection system (Amersham Pharmacia). The mouse monoclonal antibody 5D12 (mAb5D12) was produced as described previously.[7] The

A

C12orf2

B

Exon 20 FBLN1-D

CTGTGCGGCAGACCAGCCCTCAGAACCAGTACTCAGAGACGAAGATGTGGACGTTGACAACATTTCGGTGGGAGAC
CAGGCCCCCGACCACATAGTTCATCTCCAGCTTCAGGACGGCATGAAATGGGCCCACGATGGGCCGCACCTGGCGC
ACGACACCTGCGGAGAGAGCAGAAGGTGTGCTGGAAGTTAGAAGGGACTG...intron(11kb)...TATCATCG
TCATTCCTTTTTTTTTTTTTTTTTGCTAATTTTGCACAACATGCCTCTACTGCCTATGTAAAAAATAATCANGGAAGC
CATTGGCANTTTTTATAACAACTATTAAGTTATATGAAGTGTGAGTGTAGTAACCAGCTTTGGAGACAAAGTCTTC
ATTCAGGGCTATAGCAGCTGTGCAGGGAGAGCCCAGCTAATGAAAGGGGAAACTTTGGACTAACTTTCCCCTTCCT
CCAGTGGTGTTTGAAATGNGTATGTTTTCTTACATTTGCNTCNGATTTGGGGTCTGCCAGATTCTTTCTTCTTTATG
CTCTAATTTGATATTTCATATTATTTCATGACTAGGAAATTTAAGGATTTTAACATTTGGGGGCGGTATTTTCTAT
TCATAATAAAAGTAGTTTGATGTCTGGATAGATTTTTTTAAAAAAAAAATGGTTGATGGAAGCTGGTCTTGTTGCT
AAAGTAAATCTTTCTATAAATAAATGCAGAAACATCTGTGAAGGGCATAGTCTGAATGTGGCAGACATATGAATTG
CGTCAATTCCCATCTTGCGGCCAAGATTTCTTCCTTGGGCTTTCTTTATAGCTAATGTTGTGGCAAAGTTTCACAT
TCTCACAGCATTAGGCAGTAAAATGGTCAAAAGAAATGGTGCCAAGTTACCCTCTTTCTTAAGGTAGTCAGTAGTA
GGAATTTGGACTTACCAAGGAAAAGTGCCAGTGTATTTTTGGTTTTATTTTTTAGGACTNNAAGACCTNAAAGGTC
TCCTTCAACTTCAGTTTTANCCCTGGCTTTAGGCAATTTTCCAAATGTAAAGCTACTTTCAAGAAATCAGTGTGGT
ATCACAGGGAGCTGGGGTCAGTAGAAAAAGAAGACACAAAGTCTCTCCTAGAACTCCATAGGCCAATCAAATGACC
TTTTATAGAAACAACTTGAAATTCCTTTTTCAAAAGCACAAAAATGCTAATTGAAACAAACCAAACAAACCCACC
CCACAAGGACTGCAATTCAAATGCCTAAGGGGGAAGAGTGGGGACAGGGGAGGAAAATTCTTAGGAAAATTATCTG
AAGCCATACACTTGTGTTTTGCTCTTTGGTGATTGTATGTTAAAATGGAATGATTTAGTATTTTTAAGATAAAAAT
TAGCCAGGACTGTAAGAACCCTATGTACCTTTGCAGGTGCCTGTGTAGATCATCCTAGAATACCTGTGTGGTGCTG
TCCTTCCTCAAGACTACCTCATTCTCACTGGCTCGGAGACTCCTGCCTGCTGAGGTGAGTGGT

Exon 2 C12orf2

C

nl (12)   der (12)   der (22)   nl (22)   FBLN1

Figure 2 (A) A schematic representation of the various splice variants of *C12orf2* (*HoJ-1*) and *FBLN1*. The position of the breakpoint is indicated with an arrow. (B) Nucleotide sequence of the breakpoint region on the der(12). Sequences derived from chromosome 22 are underlined. Exon sequences are represented in bold. (C) Schematic representation of the normal chromosomes 12 and 22 and the two derivative chromosomes. The two genes disrupted by the t(12;22), *C12orf2* and *FBLN1*, are depicted on the normal chromosomes together with their transcriptional orientation on the chromosomes. The position of the breakpoint is indicated with a black arrow. On the derivative chromosomes, the putative fusion transcripts are depicted but as can be seen on the normal chromosomes, the orientation of both genes is such that no reciprocal fusion transcripts can be formed.

epitope of mAb5D12 antibody maps to the C-terminal region of *FBLN1-C* (residues 567-683). The rabbit polyclonal antibody (rb811) was raised against the C-terminal region of *FBLN1-D* (residues 567-703).[8]

RESULTS
The 5′UTR of *C12orf2* is disrupted by the translocation
Using a vectorette-PCR mediated approach, we isolated a 1.2 kb breakpoint encompassing *Bam*HI fragment. Sequencing of the insert showed ectopic sequences fused to known sequences (obtained during the random sequence sampling of chromosome 12p derived cosmid LL12NCO1-149H4 which spans the chromosome 12 breakpoint).[4] In fig 2B the sequence

of the breakpoint region on the der(12) is depicted. Further analysis of the chromosome 12 derived sequences showed that the breakpoint on chromosome 12p was located between two exons belonging to a cDNA contig constructed starting from the anonymous EST R72964, which in its turn was isolated with STS PD108.[4] EST R72964 corresponds to a gene designated *C12orf2* located at 12p, also known as *HoJ-1* (GenBank accession number U82396). In silico mapping of the *C12orf2* cDNA, showed that the breakpoint is located in the 5′UTR (fig 2A). At least four alternatively spliced exons were detected by sequencing intron-exon boundaries using cDNA derived sequencing primers (data not shown). Northern blot analysis showed that *C12orf2* is widely expressed as a 6.2 kb
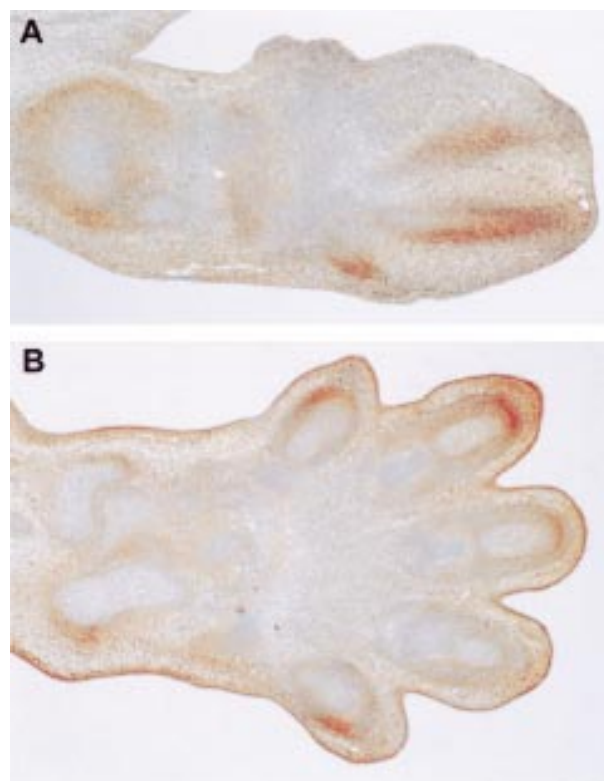
Figure 3 Northern blot analysis of total RNA from skin fibroblasts of an affected female (lane 2). Lane 1 contains RNA from control skin fibroblasts. Each lane contains 15 µg of total RNA. (A) Hybridisation with the PD108 probe (corresponding to *C12orf2/HoJ-1*). (B, C) Hybridisations using probes specific for *FBLN1-D* and *FBLN1-C*, respectively. (D) Hybridisation with the probe residing in the region common to all the *fibulin* variants. The 2.7 kb band corresponds to the *FBLN1-D* transcript, whereas the 2.4 kb band corresponds to the *FBLN1-C* transcript. (E) Hybridisation to a human β-actin cDNA probe.

Figure 4 Fbln1 is expressed in the developing murine handplate. Shown are sections of handplate regions of ~12 dpc (A) and ~13 dpc (B) mouse embryos immunohistochemically stained using rabbit anti-fibulin-1 IgG and reagents supplied in the Vectastain ABC kit (Vector Laboratories, Burlingame, CA) including horseradish peroxidase conjugated anti-antibodies and the chromogenic substrate DAB. The sections were also counterstained with Mayer's haematoxylin.

transcript.[4] A 2.2 kb alternatively spliced transcript is also expressed exclusively in testis.

FBLN1-D is disrupted by the translocation

A BLAST search conducted with the ectopic sequences (210 bases) from the 1.2 kb vectorette clone showed a 100% sequence identity with BAC CTA-941F9 (GenBank accession number Z95331), which had previously been assigned to chromosome 22q13.3.[9] BAC 941F9 was used in FISH experiments on metaphase spreads from the patients, which confirmed its localisation across the breakpoint (data not shown). To exclude the possibility that additional deletions flanking the breakpoint were present, we also determined the reciprocal breakpoint flanking sequences on the derivative chromosome 22. Sequencing of a 900 bp PCR product containing the reciprocal breakpoint and comparison with the wild type sequences obtained showed that the sequences from chromosome 12p were perfectly (that is, without any breakpoint associated deletions) fused to those derived from chromosome 22q. In this way, we could show that the translocation was truly reciprocal.

BAC CTA-941F9 contains part of the gene encoding the ECM protein FBLN1. The fibulin-1 gene consists of 20 exons. Four different fibulin-1 variants result from alternative splicing of exons 15-20 (FBLN1-A-D, GenBank accession

numbers X53741, X53742, X53743 and U01244 respectively). Exact positioning of the breakpoint within the BAC showed that it was located in the intron between the last two specific exons of the *FBLN1-D* isoform (exons 19-20) (fig 2A). In order to investigate whether the alterations in *FBLN1-D* were restricted to one allele, we also sequenced the wild type *FBLN1-D*, but no mutations could be identified.

Northern blot analysis and 3′ RACE

The chromosomal orientation of the two genes, which are both widely expressed, was such that, theoretically, the reciprocal translocation could not lead to the formation of reciprocal fusion transcripts between (sense) *C12orf2* and (sense) *FBLN1-D* (fig 2C). This was confirmed by Northern blot analysis and 3′ RACE. Northern blot analysis of RNA from patient skin fibroblasts was performed using probes specific for *C12orf2* (probe PD108), the *FBLN1-C* and *D* isoform, and a probe common to all *FBLN1* isoforms (fig 3). From these Northern blot experiments it can be concluded that compared to *FBLN1-D* expression in normal control fibroblasts, the expression of *FBLN1-D* is clearly diminished in our patient. Since no clear differences in *C12orf2* expression levels are apparent on this Northern blot, no firm conclusions can be drawn about possible alterations in the expression levels of this transcript. In these Northern blot experiments, we were also not able to identify aberrant *FBLN1* or *C12orf2* transcripts in fibroblasts from our synpolydactyly patients (data not shown). 3′ RACE analysis using the UAP-2 primer and two specific *FBLN1-D* primers also failed to show the presence of any fusion transcript.
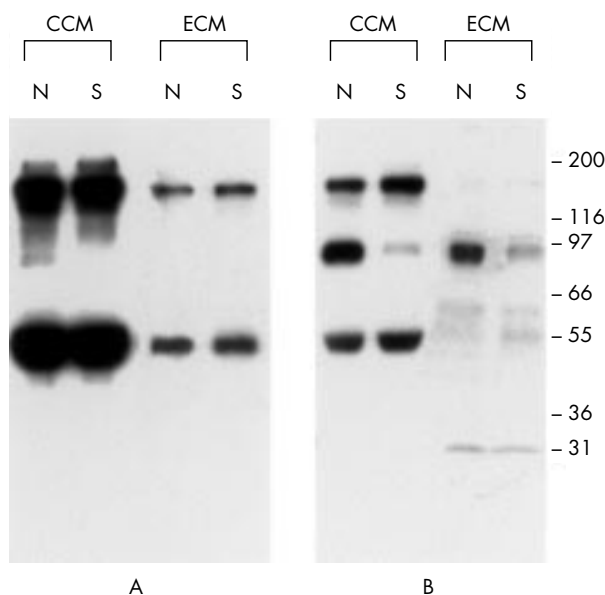
Figure 5 Immunoblot analysis of the expression of FBLN1-C and D variants by fibroblasts from subjects with t(12;22). Proteins from conditioned culture medium (CCM) and ECM EDTA extracts (ECM) obtained from normal (N) and synpolydactyly (S) fibroblasts were subjected to immunoblot analysis. Blots were stained with antibodies specific for the FBLN1-C variant (A) or the FBLN1-D variant (B).

Fbln1 is expressed in the developing limb

Human FBLN1 and mouse fibulin-1 (fbln1) are widely expressed during embryonic development.[10 11] We used immunohistochemical staining, as described by Roark et al,[12] to examine its expression in the developing mouse limb, focusing on the handplate region. As shown in fig 4, fbln1 is expressed in interdigital regions of the handplate of a ~12 dpc mouse embryo and in the lateral perichondrial regions (fig 4A). Similar staining persists in the ~13 dpc handplate, particularly in the perichondral regions and apical aspects of the developing digits (fig 4B).

FBLN1-D expression is altered in fibroblasts from a synpolydactyly patient

Skin fibroblasts derived from a t(12;22) synpolydactyly patient and a normal age matched control were grown in vitro and the level of FBLN1 incorporation into the ECMs of each was immunologically evaluated. Using antibodies specific for the C (mAb5D12) and D (rb811) variants, it was observed that FBLN1-D levels were significantly lower in extracts of the

ECM of synpolydactyly fibroblasts as compared to normal fibroblasts (fig 5). By contrast, little or no differences were apparent in the level of FBLN1-C in the ECM of synpolydactyly fibroblasts as compared to normal skin fibroblasts. The immunological analysis also indicated that FBLN1-C and D differ in the way in which each are apparently incorporated into the ECM of skin fibroblasts. While full length FBLN1-D of ~95 kDa is incorporated into the ECM, only proteolytic fragments (~55 kDa) and multimeric forms (~170 kDa) of FBLN1-C are incorporated into the ECM.

DISCUSSION

This paper describes the molecular cloning of the breakpoint of a t(12;22)(p11.2;q13.3) translocation involved in a novel complex type of synpolydactyly observed in three patients in one family. Using a positional cloning approach, we identified two genes targeted by this translocation, *FBLN1* and *C12orf2*. *C12orf2*, also known as *HoJ-1*, is located on chromosome 12p12.3. The gene is widely expressed as a 6.2 kb transcript and a 2.2 kb transcript in testis. Interestingly, the protein encoded by *C12orf2* has a 56% homology with B44478, a putative cell growth or differentiation regulator.[13] Since, at present, there is no further information regarding the function of *C12orf2*, its role in the genesis of the observed phenotype cannot be completely excluded. Since we do not have data on C12orf2 expression at the protein level, it remains difficult to speculate whether or not the expression of C12orf2 is affected by this translocation.

FBLN1 encodes a calcium binding ECM and plasma glycoprotein. Four fibulin-1 variants, designated FBLN1A-D, all differing at their carboxyl termini, are encoded by alternatively spliced transcripts.[7 8 14 15] *FBLN1-A* and *FBLN1-B* are only expressed in human placenta, whereas *FBLN1-C* and *FBLN1-D* are expressed in a variety of tissues and cultured cells. FBLN1 has been shown to interact with nidogen, NOVH, fibronectin, laminin, aggrecan, versican, tropoelastin, and amyloid precursor protein.[12 14–21] FBLN1 may also play a role in the regulation of cell migration[22] as well as in haemostasis and thrombosis owing to its ability to bind fibrinogen and incorporate into clots.[7 23 24] Expression studies in human and mouse embryos suggest a role for FBLN1 in organogenesis and embryonic development. Zhang et al[11] showed fbln1 expression in the developing mouse limb. More specifically, fbln1 was expressed in precartilage condensations of the phalanges. FBLN1 expression in human embryos was analysed by Miosge et al.[10] In human embryos of gestational week (gw) 4, FBLN1 staining was observed in the early mesenchymal bone anlagen. In embryos of gw 6.5 and 8, all perichondrial structures showed FBLN1 expression but the chondrocytes themselves showed no staining. Later in development, in embryos of gw 10,
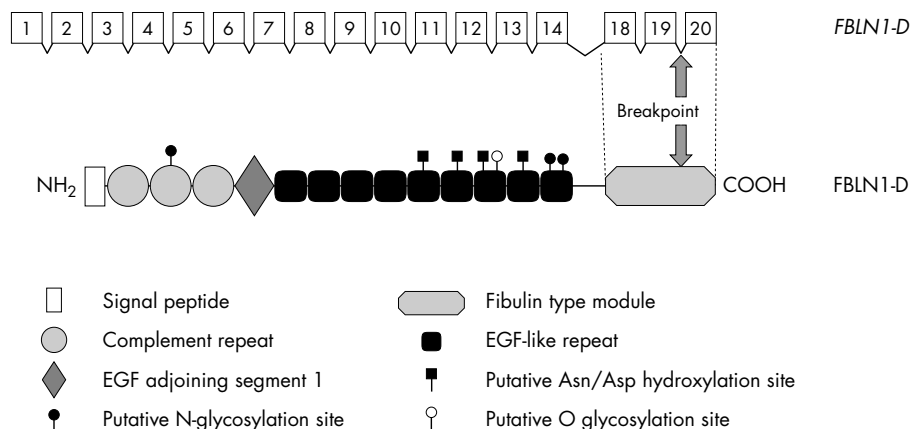
Figure 6 The t(12;22)(p11.2;q13.3) results in disruption of the "fibulin type" module of FBLN1-D. The position of the breakpoint is indicated with an arrow. The fibulin-1D gene is depicted at the top, the fibulin-1D protein at the bottom.

FBLN1 expression is prominent in the interterritorial matrix surrounding the hypertrophic chondrocytes. Our immunohistochemical stainings confirm that fbln1 is expressed in the developing handplate of mouse embryos. We observed fbln1 expression in the interdigital regions of a 12 dpc developing murine handplate and in the lateral perichondrial regions. In the 13 dpc handplate, fbln1 staining is more prominent in the apical aspects of the developing digits. The expression pattern of fbln1 in the developing handplate correlates with the phenotype observed in our patients in whom the deformities are also localised in the distal structures (metacarpals and phalanges) of the developing upper limb.

Our findings show that the t(12;22) translocation results in disruption of the "fibulin type module" of the FBLN1-D variant (fig 6). We investigated several obvious consequences of the translocation. Using RACE and Northern blot analysis no fusion transcripts were detectable in RNA preparations derived from patient fibroblasts so it is unlikely that the production of mutant proteins results in a dominant negative effect. Similarly, no aberrant polypeptides were detected in extracts of cultured patient fibroblasts. Therefore, we favour the possibility that the t(12;22) results in a haploinsufficiency for FBLN1-D. Haploinsufficiency has indeed been implicated in limb malformations. For example, deletions of a large part of the genes in the *HOXD* cluster result in monodactylous limbs and abnormal genitalia.[25] Devriendt *et al*[26] described a patient with hand-foot-genital syndrome, velopharyngeal insufficiency, and persistent patent ductus Botalli, associated with haploinsufficiency for the *HOXA* cluster. A submicroscopic deletion of chromosome 2q31 which removes the most 5′ *HOXD* genes and the adjacent *EVX2* gene results in a limb phenotype similar to synpolydactyly.[27] Other examples of hemizygosity for the *HOXD* cluster resulting from deletions of 2q31 associated with limb and genital malformations have been described.[28 29] These observations show that the presence of both alleles of certain *Hox* genes is necessary for normal growth and limb patterning. Similarly, we speculate that a diploid dose of *FBLN1-D* is necessary for normal limb morphogenesis.

Our findings show that cultured fibroblasts from patients with the t(12;22) had significantly reduced levels of FBLN1-D polypeptide incorporated in the ECM and present in the conditioned culture medium as compared to control fibroblasts. By contrast, levels of FBLN1-C were similar both in the ECM and conditioned culture medium fractions from the patient fibroblasts. The latter results are consistent with the fact that the exon encoding the FBLN1-C specific carboxy terminal module (exon 17) is upstream from the D specific exon disrupted by the translocation (exon 20). Therefore, it is predictable that the production of the C specific variant might be spared by the mutation found in this family. The basis for the reduced incorporation of FBLN1-D in synpolydactyly fibroblasts is uncertain, but may be related to quantity, and, consequently, may be the result of haploinsufficiency. However, we cannot at present rule out the possibility that the mutation results in the production of a form of FBLN1-D that is more susceptible to proteolytic degradation than the wild type polypeptide. Taken together, the results from our analysis support the hypothesis that haploinsufficiency for FBLN1-D might have caused the abnormal phenotype. It must be noted, however, that in this context the term haploinsufficiency should be used with the understanding that only loss of the D isoform is considered since no changes were observed in the expression of FBLN1-C. In the 22q13 deletion syndrome (deletion of chromosomal band 22q13.3), the whole FBLN1 cluster is contained within the deletion interval. In this syndrome the hand malformations are very mild (ranging from syndactyly to fifth finger clinodactyly or relatively fleshy hands).[30] In our patients, on the other hand, alterations in FBLN1-D expression alone seem to be responsible for the observed limb deformities. A plausible explanation for this

phenomenon might be that there is a critical balance in the stoichiometry of the different FBLN1 isoforms. We believe that the translocation might result in a disturbance of this critical balance and lead to the observed phenotype.

The formation of the digits is a complex, tightly regulated process which involves apoptosis and in which several pathways and signalling molecules are involved. Solursh *et al*[31–33] and Archer *et al*[34] showed that the ECM plays an important role in determining the fate of cells in the interdigital region during morphogenesis. Surgical manipulations of the interdigital tissue of the chick embryo leg bud result in the formation of ectopic digits.[35] Miner *et al*[36] showed that mice lacking the laminin α5 chain exhibit multiple developmental defects, including exencephaly and syndactyly. Mutations in the fibrillin-2 gene, which results in congenital contractural arachnodactyly (CCA, MIM 121050) in humans, can cause syndactyly in mice.[37–39] These data show that a "deficient" ECM can lead to anomalous limb development, both in humans and in mice. We believe that haploinsufficiency of FBLN1-D results in similar ECM changes and causes the observed synpolydactyly.

To our knowledge, this is the first human disorder linked to alterations in *FBLN1*. Corroboration of this conclusion requires that mutations in this gene are found in other families with complex synpolydactyly. In this regard, Percin *et al*[40] have described a Turkish family with a complex type of syndactyly and synostoses. In this family, *HOXD13* involvement was excluded. Furthermore, linkage analysis, using polymorphic markers of the region involved on chromosomes 12p and 22q turned out to be negative (A N Akarsu, personal communication; data not shown). Therefore, the genetic defects in the Turkish family and the family described in the present study appear different. Alternative proof that *FBLN1* mutations may indeed cause hand and foot malformations may be obtained by the construction of a *FBLN1-D* specific knock-out mouse and by analysis of its phenotype. Recently, Kostka *et al*[41] described the phenotype of fibulin-1 deficient mice. Heterozygous embryos developed normally and were phenotypically indistinguishable from wild type litter mates. The homozygous embryos all died in the perinatal period because of massive haemorrhages in several tissues. The cause of the early death was probably kidney and lung defects combined with abnormalities in some endothelial compartments. These mice were deficient for all the fibulin-1 isoforms and no limb deformities were mentioned. We are currently constructing a *FBLN1-D* specific knock-out in order to find out whether an isoform specific knock-out mouse develops limb abnormalities and whether a critical dose of FBLN1-D is essential for proper limb development. The involvement of FBLN1-D in a specific human disorder might also shed light on functions of the FBLN1 isoforms, which are currently poorly understood.

. . . .
Authors' affiliations
P Debeer, E F P M Schoenmakers, J-P Fryns, W J M Van de Ven, Centre for Human Genetics, Herestraat 49, B-3000 Leuven, Belgium
P Debeer, E F P M Schoenmakers, W J M Van de Ven, Flanders Interuniversity Institute for Biotechnology, Leuven, Belgium

W O Twal, W S Argraves, Department of Cell Biology and Anatomy, Medical University of South Carolina, Charleston, SC, USA
L De Smet, Department of Orthopaedic Surgery, University Hospital Pellenberg, Weligerveld 1, B-3212 Pellenberg, Belgium

REFERENCES

1 **De Smet L**, Debeer P, Fryns JP. Cenani-Lenz syndrome in father and daughter. *Genet Couns* 1996;**7**:153-7.
2 **Debeer P**, Schoenmakers EF, De Smet L, Van de Ven WJ, Fryns JP. Co-segregation of an apparently balanced reciprocal t(12;22)(p11.2;q13.3) with a complex type of 3/3'/4 synpolydactyly associated with metacarpal, metatarsal, and tarsal synostoses in three family members . *Clin Dysmorphol* 1998;**7**:225-8.
3 **Debeer P**, Schoenmakers EF, Thoelen R, Fryns JP, Van de Ven WJ. Physical mapping of the t(12;22) translocation breakpoints in a family with a complex type of 3/3'/4 synpolydactyly. *Cytogenet Cell Genet* 1998;**81**:229-34.
4 **Debeer P**, Schoenmakers EF, Thoelen R, Holvoet M, Kuittinen T, Fabry G, Fryns JP, Goodman FR Van de Ven WJM. Physical map of a 1.5 Mb region on 12p11.2 harbouring a synpolydactyly associated chromosomal breakpoint. *Eur J Hum Genet* 2000;**8**:561-70.
5 **Schoenmakers EF**, Mols R, Wanschura S, Kools PF, Geurts JM, Bartnitzke S, Bullerdiek J, Van den Berghe H, Van de Ven WJM. Identification, molecular cloning, and characterization of the chromosome 12 breakpoint cluster region of uterine leiomyomas. *Genes Chrom Cancer* 1994;**11**:106-18.
6 **Schoenmakers EF**, Geurts JM, Kools PF, Mols R, Huysmans C, Bullerdiek J, Van den Berghe H, Van de Ven WJM. A 6-Mb yeast artificial chromosome contig and long-range physical map encompassing the region on chromosome 12q15 frequently rearranged in a variety of benign solid tumors. *Genomics* 1995;**29**:665-78.
7 **Argraves WS**, Tran H, Burgess WH, Dickerson K. Fibulin is an extracellular matrix and plasma glycoprotein with repeated domain structure. *J Cell Biol* 1990;**111**:3155-64.
8 **Tran H**, Mattei M, Godyna S, Argraves WS. Human fibulin-1D: molecular cloning, expression and similarity with S1-5 protein, a new member of the fibulin gene family. *Matrix Biol* 1997;**15**:479-93.
9 **Korenberg JR**, Chen XN, Tran H, Argraves WS. Localization of the human gene for fibulin-1 (FBLN1) to chromosome band 22q13.3. *Cytogenet Cell Genet* 1995;**68**:192-3.
10 **Miosge N**, Gotz W, Sasaki T, Chu ML, Timpl R, Herken R. The extracellular matrix proteins fibulin-1 and fibulin-2 in the early human embryo. *Histochem J* 1996;**28**:109-16.
11 **Zhang HY**, Timpl R, Sasaki T, Chu ML, Ekblom P. Fibulin-1 and fibulin-2 expression during organogenesis in the developing mouse embryo. *Dev Dyn* 1996;**205**:348-64.
12 **Roark EF**, Keene DR, Haudenschild CC, Godyna S, Little CD, Argraves WS. The association of human fibulin-1 with elastic fibers: an immunohistological, ultrastructural, and RNA study. *J Histochem Cytochem* 1995;**43**:401-11.
13 **Weitzel JN**, Kasperczyk A, Mohan C, Krontiris TG. The HRAS1 gene cluster: two upstream regions recognizing transcripts and a third encoding a gene with a leucine zipper domain. *Genomics* 1992;**14**:309-19.
14 **Pan TC**, Kluge M, Zhang RZ, Mayer U, Timpl R, Chu ML. Sequence of extracellular mouse protein BM-90/fibulin and its calcium- dependent binding to other basement-membrane ligands. *Eur J Biochem* 1993;**215**:733-40.
15 **Tran H**, VanDusen WJ, Argraves WS. The self-association and fibronectin-binding sites of fibulin-1 map to calcium-binding epidermal growth factor-like domains. *J Biol Chem* 1997;**272**:22600-6.
16 **Aspberg A**, Adam S, Kostka G, Timpl R, Heinegard D. Fibulin-1 is a ligand for the C-type lectin domains of aggrecan and versican. *J Biol Chem* 1999;**274**:20444-9.
17 **Balbona K**, Tran H, Godyna S, Ingham KC, Strickland DK, Argraves WS. Fibulin binds to itself and to the carboxyl-terminal heparin-binding region of fibronectin. *J Biol Chem* 1992;**267**:20120-5.
18 **Ohsawa I**, Takamura C, Kohsaka S. Fibulin-1 binds the amino-terminal head of beta-amyloid precursor protein and modulates its physiological function. *J Neurochem* 2001;**76**:1411-20.
19 **Perbal B**, Martinerie C, Sainson R, Werner M, He B, Roizman B. The C-terminal domain of the regulatory protein NOVH is sufficient to promote interaction with fibulin 1C: a clue for a role of NOVH in cell-adhesion signaling. *Proc Natl Acad Sci USA* 1999;**96**:869-74.
20 **Sasaki T**, Kostka G, Gohring W, Wiedemann H, Mann K, Chu ML, Timpl R. Structural characterization of two variants of fibulin-1 that differ in nidogen affinity. *J Mol Biol* 1995;**245**:241-50.
21 **Talts JF**, Andac Z, Gohring W, Brancaccio A, Timpl R. Binding of the G domains of laminin alpha1 and alpha2 chains and perlecan to heparin, sulfatides, alpha-dystroglycan and several extracellular matrix proteins. *EMBO J* 1999;**18**:863-70.
22 **Qing J**, Maher VM, Tran H, Argraves WS, Dunstan RW, McCormick JJ. Suppression of anchorage-independent growth and matrigel invasion and delayed tumor formation by elevated expression of fibulin-1D in human fibrosarcoma-derived cell lines. *Oncogene* 1997;**15**:2159-68.
23 **Kluge M**, Mann K, Dziadek M, Timpl R. Characterization of a novel calcium-binding 90-kDa glycoprotein (BM-90) shared by basement membranes and serum. *Eur J Biochem* 1990;**193**:651-9.
24 **Tran H**, Tanaka A, Litvinovich SV, Medved LV, Haudenschild CC, Argraves WS. The interaction of fibulin-1 with fibrinogen. A potential role in hemostasis and thrombosis. *J Biol Chem* 1995;**270**:19458-64.
25 **Del Campo M**, Jones MC, Veraksa AN, Curry CJ, Jones KL, Mascarello JT, Ali-Kahn-Catts Z, Drumheller T, McGinnis W. Monodactylous limbs and abnormal genitalia are associated with hemizygosity for the human 2q31 region that includes the HOXD cluster. *Am J Hum Genet* 1999;**65**:104-10.
26 **Devriendt K**, Jaeken J, Matthijs G, Van Esch H, Debeer P, Gewillig M, Fryns JP. Haploinsufficiency of the HOXA gene cluster in a patient with hand-foot-genital syndrome, velopharyngeal insufficiency, and persistent patent ductus Botalli. *Am J Hum Genet* 1999;**65**:249-51.
27 **Goodman FR**, Majewski F, Winter R, Scambler P. Haploinsufficiency for HOXD8-HOXD13 and EVX2 causes atypical synpolydactly. *Am J Hum Genet* 1999;**65**(suppl):A298.
28 **Nixon J**, Oldridge M, Wilkie AO, Smith K. Interstitial deletion of 2q associated with craniosynostosis, ocular coloboma, and limb abnormalities: cytogenetic and molecular investigation. *Am J Med Genet* 1997;**70**:324-7.
29 **Slavotinek A**, Schwarz C, Getty JF, Stecko O, Goodman F, Kingston H. Two cases with interstitial deletions of chromosome 2 and sex reversal in one. *Am J Med Genet* 1999;**86**:75-81.
30 **Phelan MC**, Rogers RC, Saul RA, Stapleton GA, Sweet K, McDermid H, Shaw SR, Claytor J, Willis J, Kelly DP. 22q13 deletion syndrome. *Am J Med Genet* 2001;**101**:91-9.
31 **Solursh M**. Cell-matrix interactions during limb chondrogenesis. *Prog Clin Biol Res* 1984;**151**:47-60.
32 **Solursh M**. Ectoderm as a determinant of early tissue pattern in the limb bud. *Cell Differ* 1984;**15**:17-24.
33 **Solursh M**, Jensen KL, Zanetti NC, Linsenmayer TF, Reiter RS. Extracellular matrix mediates epithelial effects on chondrogenesis in vitro. *Dev Biol* 1984;**105**:451-7.
34 **Archer CW**, Rooney P, Wolpert L. Cell shape and cartilage differentiation of early chick limb bud cells in culture. *Cell Differ* 1982;**11**:245-51.
35 **Hurle JM**, Colombatti A. Extracellular matrix modifications in the interdigital spaces of the chick embryo leg bud during the formation of ectopic digits. *Anat Embryol* 1996;**193**:355-64.
36 **Miner JH**, Cunningham J, Sanes JR. Roles for laminin in embryogenesis: exencephaly, syndactyly, and placentopathy in mice lacking the laminin alpha5 chain. *J Cell Biol* 1998;**143**:1713-23.
37 **Putnam EA**, Zhang H, Ramirez F, Milewicz DM. Fibrillin-2 (FBN2) mutations result in the Marfan-like disorder, congenital contractural arachnodactyly. *Nat Genet* 1995;**11**:456-8.
38 **Wang MT**, Godfrey M. Fibrillin-2 (FBN2) mutation in congenital contractural arachnodactyly. *Am J Hum Genet* 1995;**57**:A231.
39 **Chaudhry SS**, Gazzard J, Baldock C, Dixon J, Rock MJ, Skinner GC, Steel KP, Kielty CM, Dixon MJ. Mutation of the gene encoding fibrillin-2 results in syndactyly in mice. *Hum Mol Genet* 2001;**10**:835-43.
40 **Percin EF**, Percin S, Egilmez H, Sezgin I, Ozbas F, Akarsu AN. Mesoaxial complete syndactyly and synostosis with hypoplastic thumbs: an unusual combination or homozygous expression of syndactyly type I? *J Med Genet* 1998;**35**:868-74.
41 **Kostka G**, Giltay R, Bloch W, Addicks K, Timpl R, Fassler R, Chu ML. Perinatal lethality and endothelial cell abnormalities in several vessel compartments of fibulin-1-deficient mice. *Mol Cell Biol* 2001;**20**:7025-34.